Supporting Information

Highly Efficient Non-doped Blue Fluorescent OLEDs with Low Efficiency Roll-off Based on Hybridized Local and Charge Transfer Excited State Emitters

Xianhao Lv,‡[a] Mizhen Sun,‡[a] Lei Xu,[a] Runzhe Wang,[a] Huayi Zhou,[a] Yuyu Pan,[b] Qikun Sun,[a] Shitong Zhang,[c] Shanfeng Xue,*[a] and Wenjun Yang[a]

[a]Key Laboratory of Rubber-Plastics of the Ministry of Education/Shandong Province (QUST), School of Polymer Science & Engineering, Qingdao University of Science &Technology, 53-Zhengzhou Road, Qingdao 266042, P. R. China.

[b]School of Petrochemical Engineering, Shenyang University of Technology, 30 Guanghua Street, Liaoyang, 111003, P. R. China.

[c]State Key Laboratory of Supramolecular Structure and Materials, Jilin University, Changchun, 130012, P. R. China.

‡ Xianhao Lv and Mizhen Sun contributed equally to this work.

*Corresponding author E-mail: sfxue@qust.edu.cn

Contents

SI-1 Measurements

Photophysical Measurements. UV−vis absorption spectra were recorded on a Hitachi U-4100 spectrophotometer. Fluorescence measurements were recorded on a Hitachi F-4600 spectrophotometer. The influence of solvent environment on the optical property of TPAAnPI can be understood using the Lippert-Mataga equation, a model that describes the interactions between the solvent and the dipole moment of solute:

$$hc(\nu_a - \nu_f) = hc(\nu_a^0 - \nu_f^0) + \frac{2(\mu_e - \mu_g)^2}{a^3} f(\varepsilon, n)$$

Formula S1

where f is the orientational polarizability of solvents, μe is the excited-state dipole moment, μg is the ground-state dipole moment; a is the solvent cavity (Onsager) radius, derived from the Avogadro number (N), molecular weight (M), and density (d=1.0 g/cm^3); ε and n are the solvent dielectric and the solvent refractive index, respectively; f(ε,n) and a can be calculated respectively as follows:

$$f(\varepsilon, n) = \frac{\varepsilon - 1}{2\varepsilon + 1} - \frac{n^2 - 1}{2n^2 + 1}, \quad a = (3M / 4N\pi d)^{1/3}$$

The photoluminescence quantum yields (PLQY, Φ) in solution, solid film state were measured by an FLS980 spectrometer. The lifetimes (τ) of solid state and film state were measured on an Edinburgh FLS-1000 spectrometer with an EPL-375 optical laser. Since:

$$\tau = \frac{1}{Kr + Knr}$$

and

$$\phi = \frac{Kr}{Kr + Knr}$$

where τ is the lifetime, k_{nr} and k_r are the nonradiative decay rate constant and radiative decay rate constant, respectively. Φ is the PLQY. We conclude that:

$$Kr = \frac{\phi}{\tau}$$ Formula S2

Electrochemical Measurements. Cyclic voltammetry (CV) was performed with a BAS 100W Bioanalytical Systems, using a glass carbon disk (Φ= 3 mm) as the working electrode, a platinum wire as the auxiliary electrode with a porous ceramic wick, Ag/Ag+ as the reference electrode, standardized for the redox couple ferricinium/ferrocene. The procedure was performed at room temperature and a nitrogen atmosphere was maintained over the solution during measurements. The energy levels of HOMO and LUMO are calculated according to:

$$\text{HOMO} = -\left(E_{ox} \text{ vs. } Ag/Ag^{+} - E1/2^{+} \text{ vs. } Ag/Ag^{+} + 4.8\right) \text{eV};$$
$$\text{LUMO} = -\left(E_{red} \text{ vs. } Ag/Ag^{+} - E1/2^{-} \text{ vs. } Ag/Ag^{+} + 4.8\right) \text{eV}.$$ Formula S3

where the Eox vs. Ag/Ag^{+} and Ered vs. Ag/Ag^{+} are oxidation and reduction onset potentials relative to Ag/Ag^{+} electrode, respectively. $E1/2^{+}$ vs. Ag/Ag^{+} and $E1/2^{-}$ vs. Ag/Ag^{+} are half wave potentials of Fc^{+} /Fc^{-} obtained from positive and negative CV scans, respectively.

Thermal Stability Measurements. Thermal gravimetric analysis was undertaken on a Perkin-Elmer thermal analysis system from 30 to 650 °C at a heating rate of 10 K/min and a nitrogen flow rate of 80 mL/min. Differential scanning calorimetry (DSC) analysis was carried out using a NETZSCH (DSC-204) instrument from 30 to 410 °C at a heating rate of 10 K/min while flushing with nitrogen.

Density Functional Theory (DFT) calculation. All DFT calculations were carried out with the Gaussian 09 B.01 Package at the level of M062X/6-31+G(d,p), a

commonly used level for the precise geometry optimization. The ground state (S_0) and excited states of TPAAnPI are then calculated in good agreement with the experimental UV and PL data in hexane. The hexane polarity is very weak, and it can be compared well with the vacuum circumstances.

The efficiency roll-off of the non-doped EL device. The calculation formula of efficiency roll-off is as follows:

$$\eta = \frac{EQE\max - EQE1000}{EQE\max} \qquad \text{Formula S4}$$

Where EQE_{1000} is the EQE value when luminance is 1000 cd m $^{-2}$.

EQE measurement method for the non-doped device. The measured parameters included luminance, current and EL spectrum. EQE was calculated according to the formula below:

$$EQE = \frac{\pi \cdot L \cdot e}{683 \cdot I \cdot h \cdot c} \cdot \frac{\int_{380}^{780} I(\lambda) \cdot \lambda d\lambda}{\int_{380}^{780} I(\lambda) \cdot K(\lambda) d\lambda} \qquad \text{Formula S5}$$

where L (cd m^{-2}) is the total luminance of device, I (A) is the current flowing into the EL device, λ (nm) is EL wavelength, $I(\lambda)$ is the relative EL intensity at each wavelength and obtained by measuring the EL spectrum, $K(\lambda)$ is the Commision International de L'Eclairage chromaticity (CIE) standard photopic efficiency function, e is the charge of an electron, h is the Planck's constant, c is the velocity of light.

SI-2 Synthesis Section

Syntnesis of PPI-Br*:* A mixture of 9,10-phenanthraquinone (2.00 g, 9.61 mmol),

phenylamine (3.58 g, 38.42 mmol), 4-bromobenzaldehyde (1.78 g, 9.61 mmol), ammonium acetate (3.70 g, 48.03 mmol), and acetic acid (30 ml) was refluxed for 2 h under nitrogen. After cooling down, the solid product was filtrated and washed with 30 ml 1:1 water/acetic acid and 30 mL water successively, dissolved in CH_2Cl_2 and dried in $MgSO_4$, purified by thin layer chromatography and the white solid product was obtained. (3.80 g, 88.0 %). ^{1}H NMR (500 MHz, Chloroform-*d*) δ= 8.78 (dd, J = 8.0, 1.3 Hz, 1H), 8.69 (d, J = 8.4 Hz, 1H), 8.63 (d, J = 8.3 Hz, 1H), 7.67 (dd, J = 14.8, 1.0 Hz, 1H), 7.62 – 7.49 (m, 4H), 7.44 (td, J = 7.7, 7.2, 1.5 Hz, 3H), 7.40 – 7.32 (m, 4H), 7.24 – 7.15 (m, 2H), 7.10 (dd, J = 8.3, 1.2 Hz, 1H).

Synthesis of PPIB*:* PPI-Br (2.93g, 6.53mmol), bis(pinacolato)diboron (1.99 g, 7.84 mmol), Pd(dppf)Cl_2 (0.10 g, 0.13 mmol) and KOAc (1.92 g, 19.60 mmol) in degassed 1, 4-dioxane (30 ml) was stirred under N_2 at 90 ^{o}C for 8 hours. The reaction was quenched by deionized water, and the resulting mixture was washed with dichloromethane. The organic layers were collected, dried with $MgSO_4$, and concentrated in vacuum. It was purified via silica gel chromatography by petroleum ether/dichloromethane (2:1; v/v) to give the desired compound as a white solid in 80 % yield (2.65 g). ^{1}H NMR (500 MHz, Chloroform-*d*) δ= 8.88 (dd, J = 8.0, 1.5 Hz, 1H), 8.76 (d, J = 8.4 Hz, 1H), 8.70 (d, J = 8.3 Hz, 1H), 7.73 (dd, J = 15.2, 7.6 Hz, 3H), 7.68 – 7.54 (m, 5H), 7.50 (ddt, J = 5.8, 3.6, 1.9 Hz, 3H), 7.28 – 7.22 (m, 2H), 7.20 – 7.15 (m, 1H), 1.34 (d, J = 1.6 Hz, 12H).

***Synthesis of PIAN-Br**:* A mixture of PPIB (2.65 g, 5.35 mmol), 9,10-dibromoanthracene (1.5 g, 4.46 mmol), K_2CO_3 (0.9 g, 6.51 mmol), tetrahydrofuran (THF, 50 ml) and deionized water (H_2O, 10 ml), with $Pd(PPh_3)_4$ (0.15 g, 0.130 mmol) acting as catalyst was refluxed at 70 °C for 24 h under nitrogen. After the mixture was cooled down, 50 ml deionized water was added to the resulting solution and the mixture was extracted with dichloromethane for several times. The organic phase was dried over $MgSO_4$. After filtration and solvent evaporation, the given residue was purified through silica gel column chromatography using dichloromethane/petroleum ether (3:1; v/v) as eluent to give the product as light yellow solid (1.92 g, 68.8%). ^{1}H NMR (500 MHz, Chloroform-*d*) δ= 8.94 (dd, J = 8.0, 1.4 Hz, 1H), 8.81 (d, J = 8.4 Hz, 1H), 8.75 (d, J = 8.3 Hz, 1H), 8.61 (d, J = 8.8 Hz, 2H), 7.85 – 7.75 (m, 3H), 7.73 – 7.65 (m, 6H), 7.65 – 7.58 (m, 3H), 7.56 (ddd, J = 15.4, 8.4, 1.3 Hz, 2H), 7.42 – 7.28 (m, 5H).

SI-3 Supporting Figures

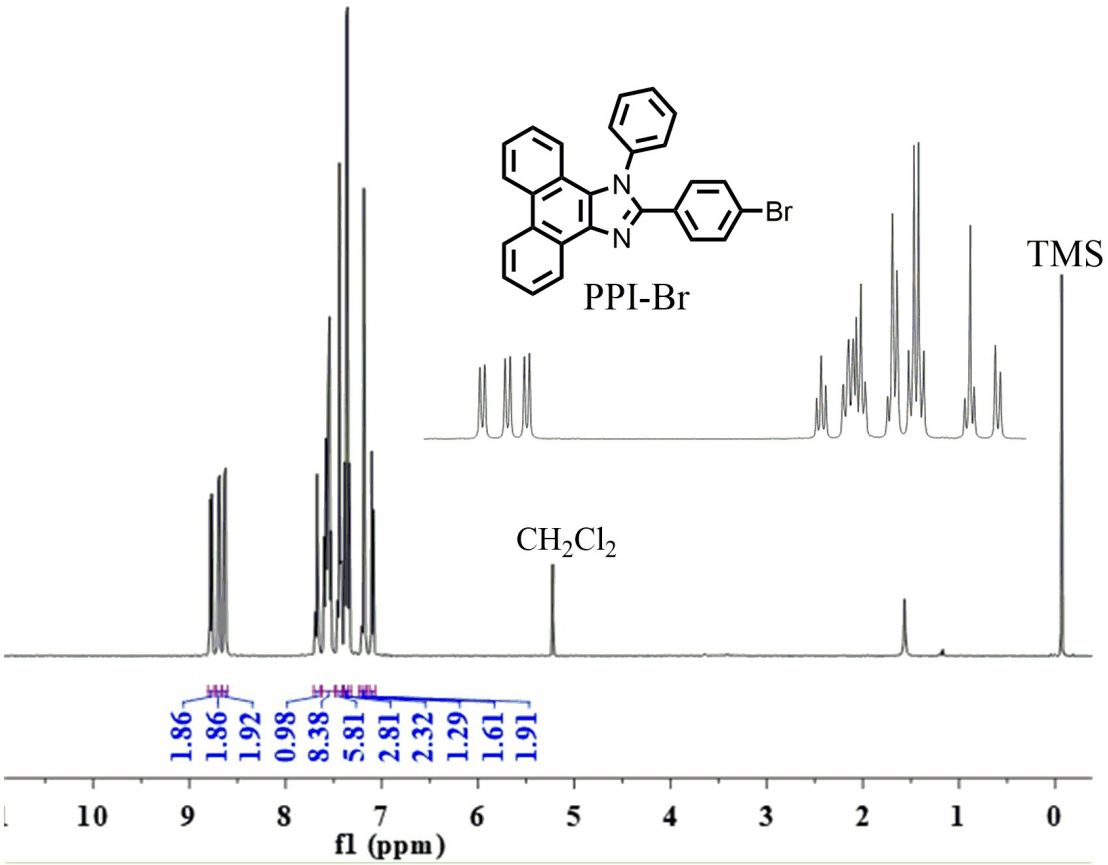

Fig. S1 ^{1}H-NMR Spectrum of PPI-Br in $CDCl_3$.

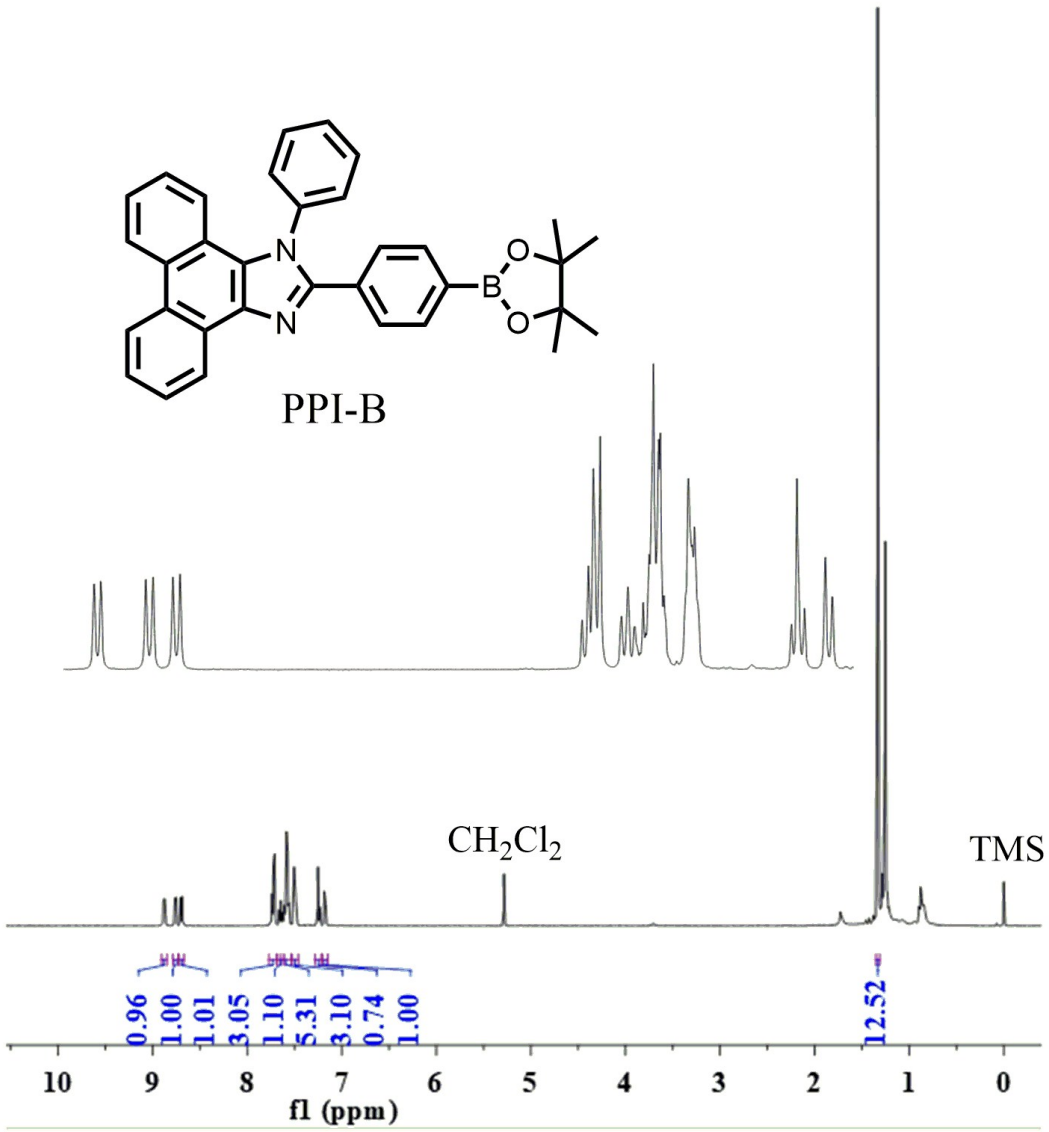

Fig. S2 ^{1}H-NMR Spectrum of PPI-B in $CDCl_3$.

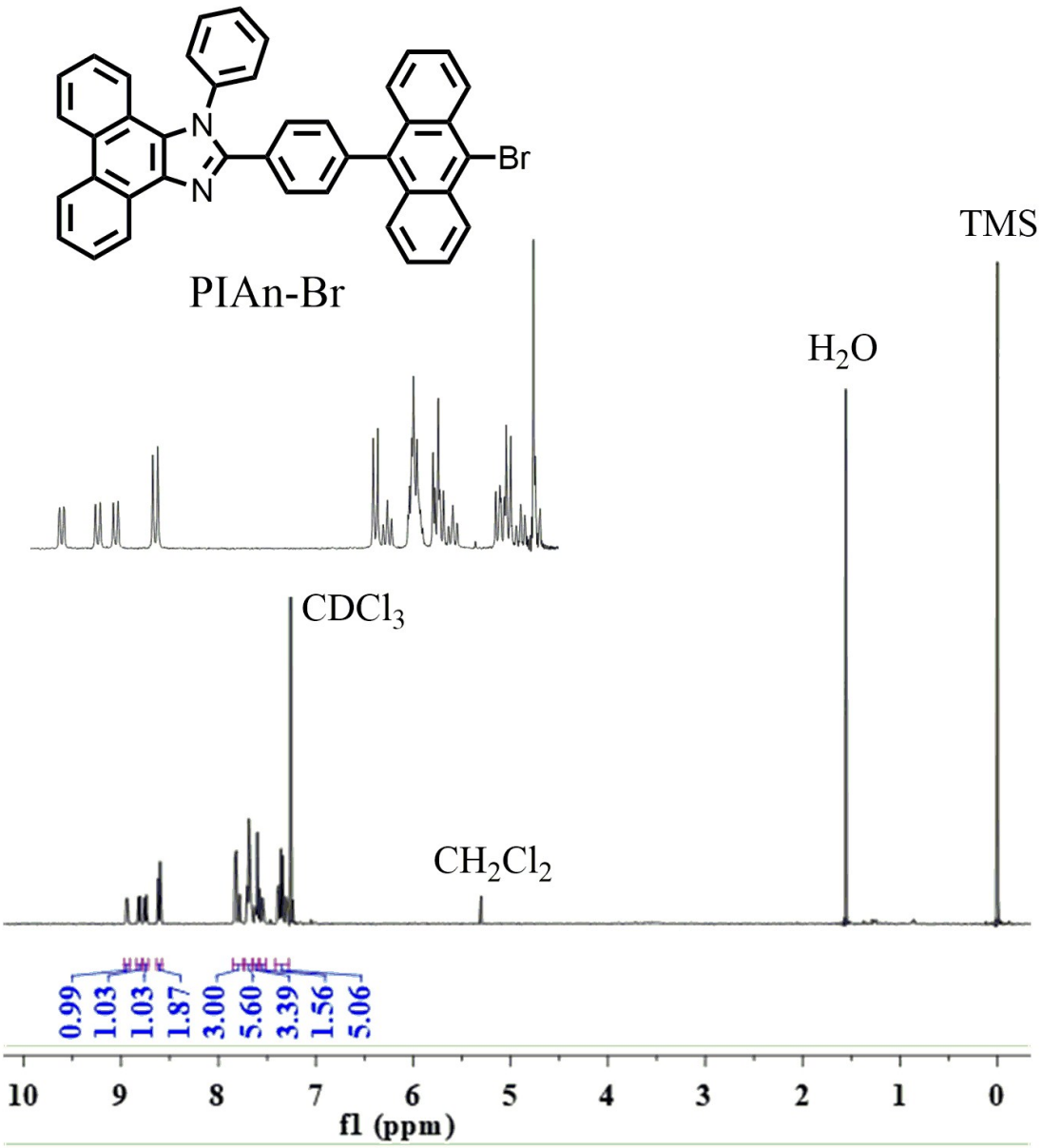

Fig. S3 ^{1}H-NMR Spectrum of PIAn-Br in $CDCl_3$.

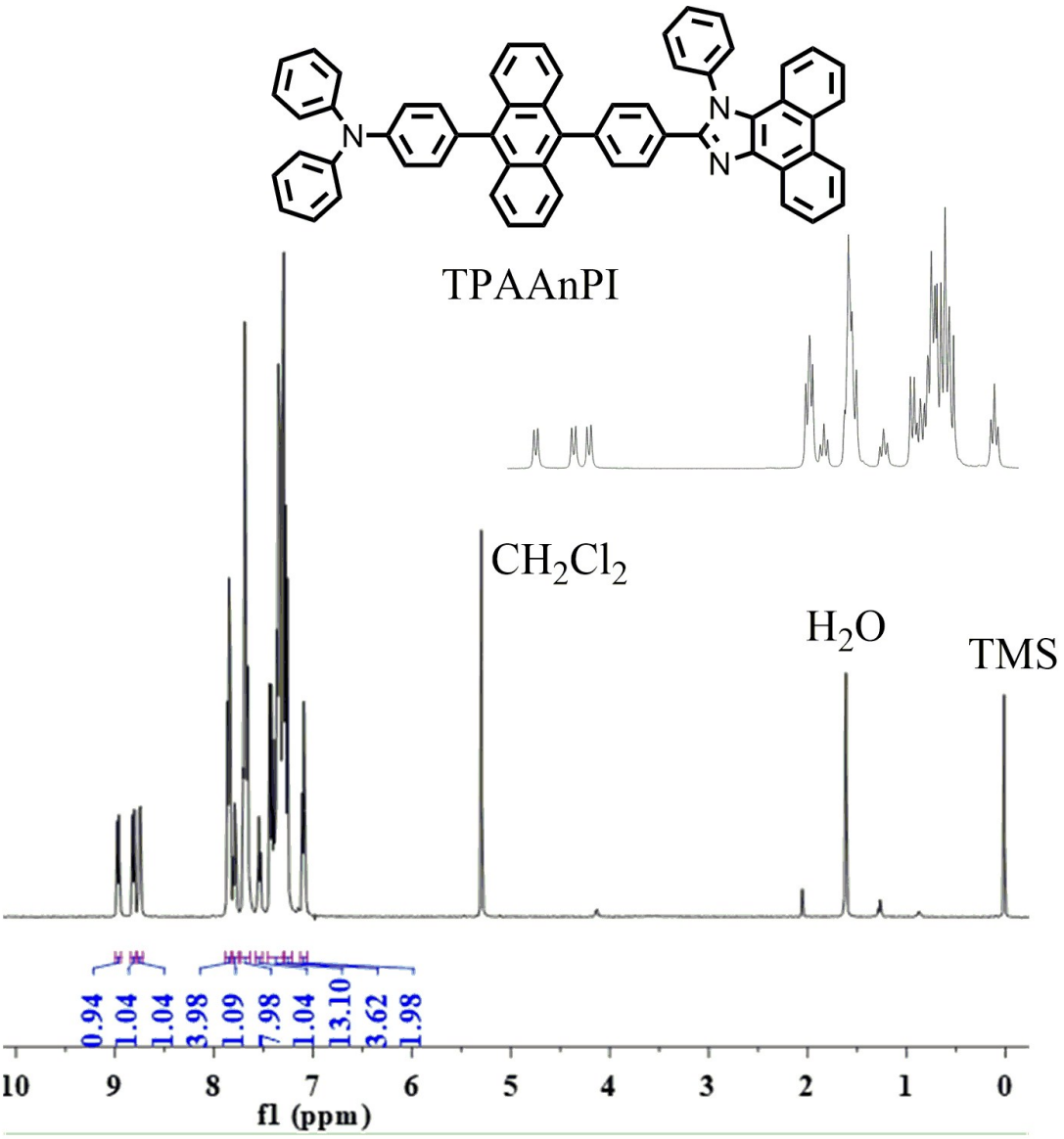

Fig. S4 ^{1}H-NMR Spectrum of TPAAnPI in $CDCl_3$.

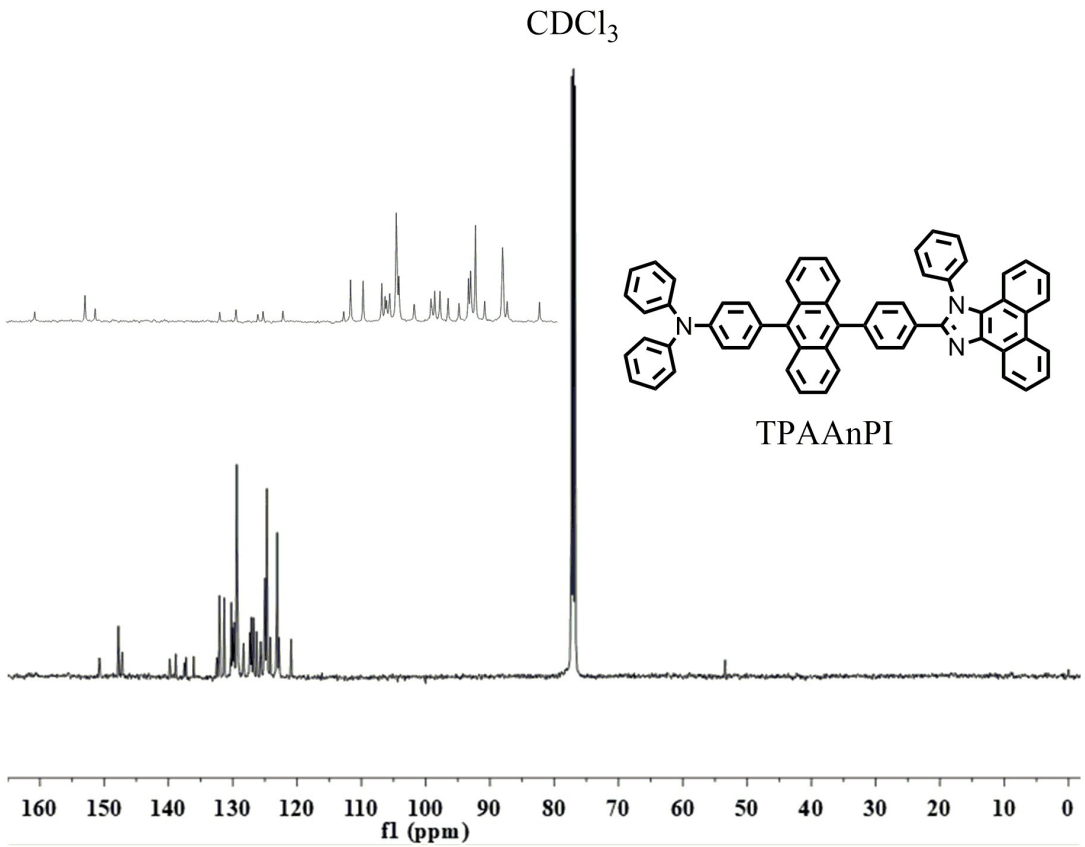

Fig. S5 ^{13}C-NMR Spectrum of TPAAnPI in $CDCl_3$.

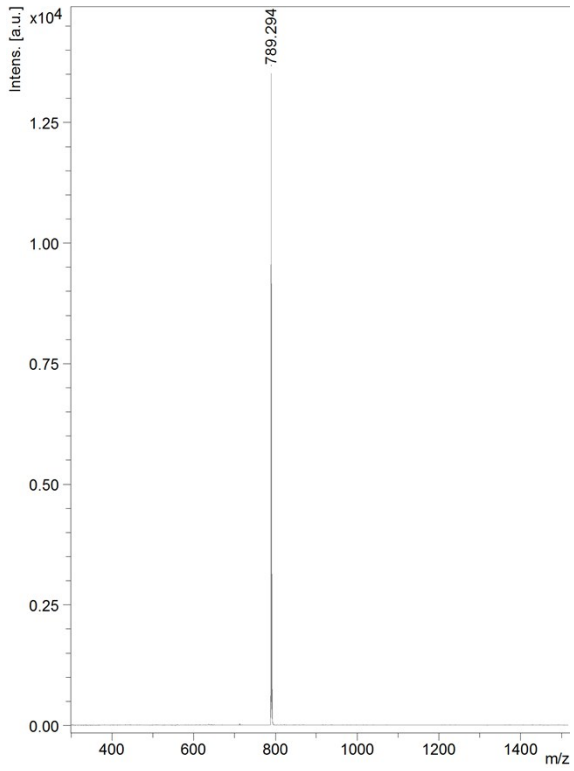

Fig. S6 Mass Spectrum (M+H+) of TPAAnPI.

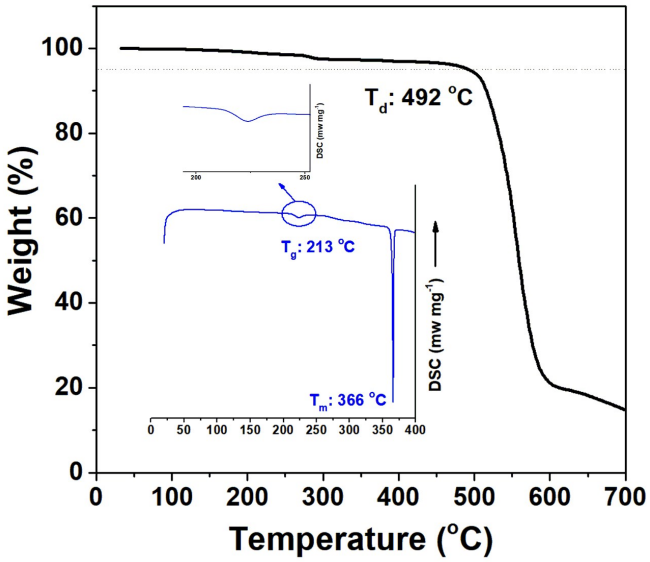

Fig. S7 Thermogravimetric analysis (TGA) of TPAAnPI, the inset is differential scanning calorimetry (DSC) curve of TPAAnPI.

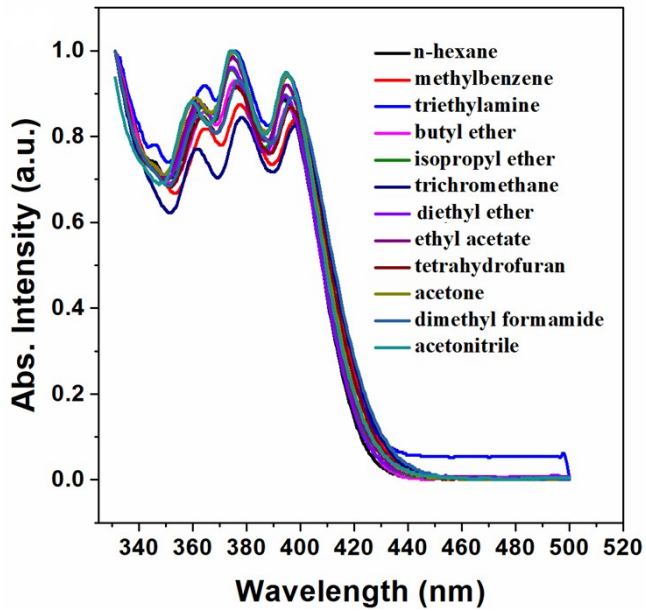

Fig. S8 Normalized UV-vis spectrum of TPAAnPI in different polarity solvents.

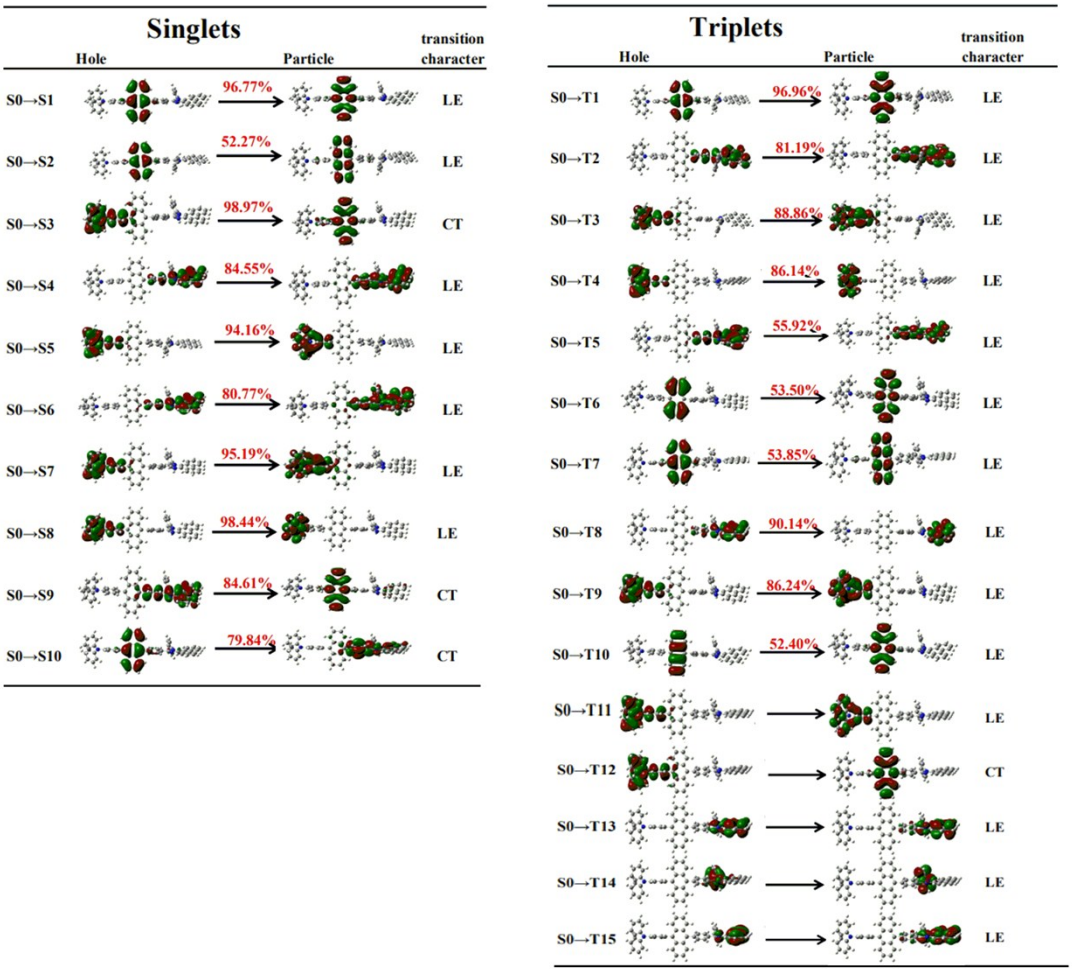

Fig. S9 The NTOs for the excited states of TPAAnPI at the M062X/6-31+G(d,p) level.

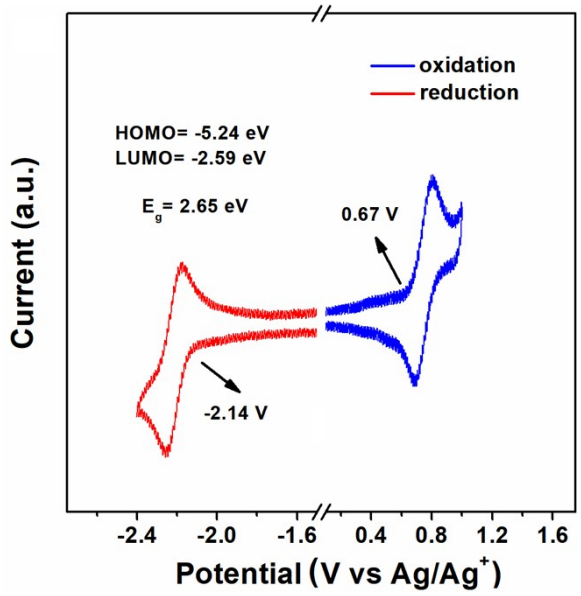

Fig. S10 CV curve of TPAAnPI.

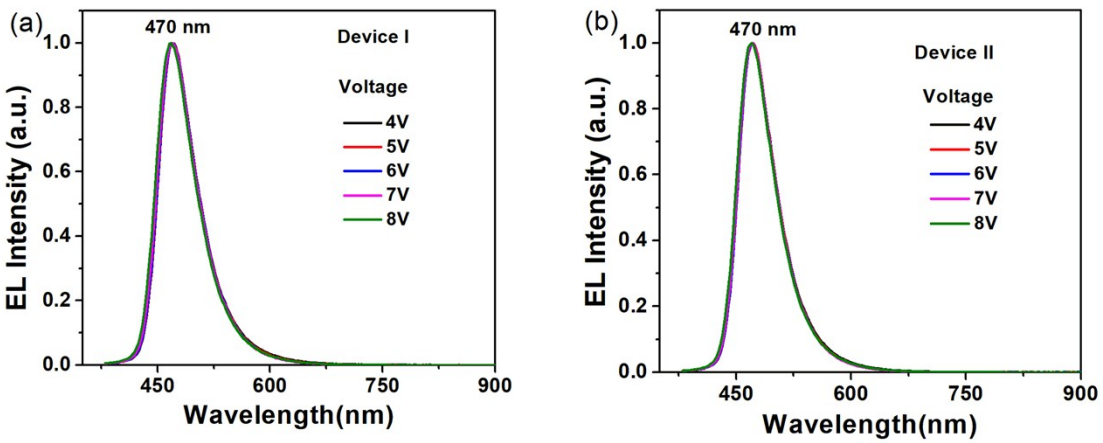

Fig. S11 (a) Normalized EL spectra of Device I at different voltages. (b) Normalized EL spectra of Device II at different voltages.

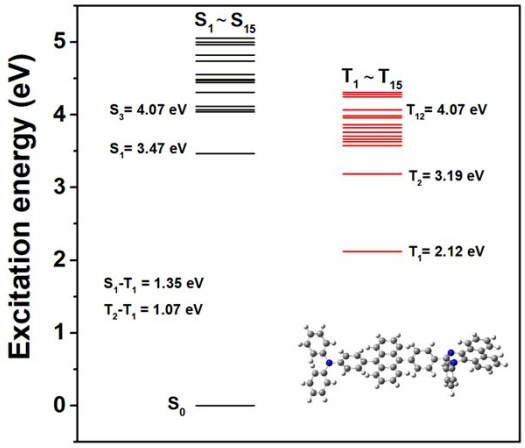

Fig. S12 Excited state (singlet and triplet) energy diagram of TPAAnPI at the geometry of S_0 state.

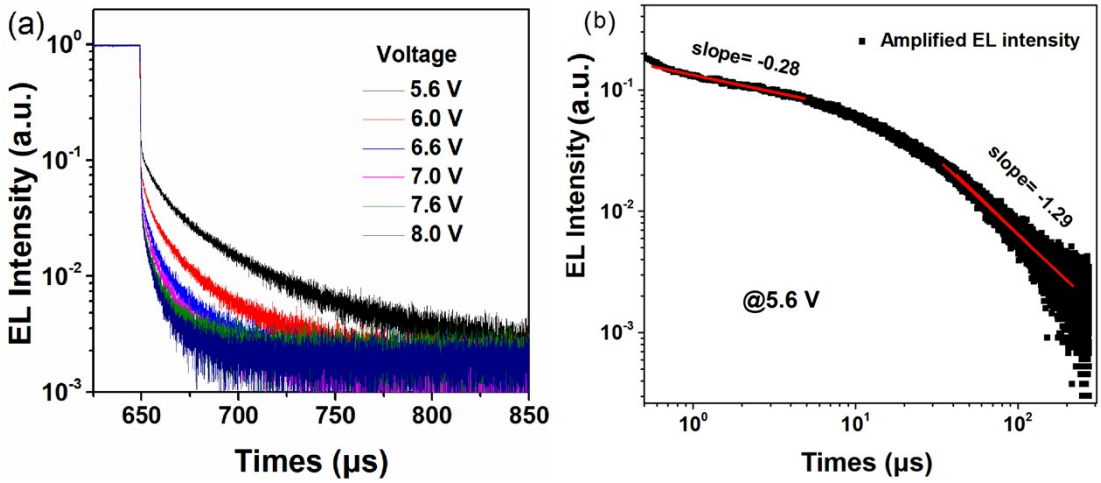

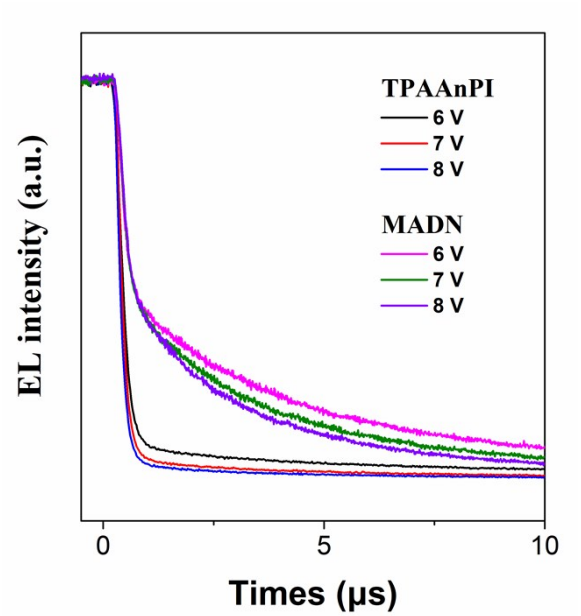

Fig. S13 (a) The transient EL decay curves of Device II at different voltages. (b) Amplified EL decay of the delayed component of Device II at 5.6 V. (c) Transient EL decay curves of TPAAnPI (Device II) and MADN-based devices (EML: mCP:10% MADN).

SI-4 Supporting Tables

Table S1 The summary photoluminescence data of TPAAnPI in different solvents.

Solvents	n-hexane	triethylamine	n-butyl ether	isopropyl ether	diethyl ether	ethyl acetate	tetrahydrofuran	acetone	acetonitrile
f[a)]	0.001	0.05	0.096	0.145	0.167	0.2	0.21	0.284	0.305
λ_{abs} (nm)[b)]	394	395	396	394	394	395	396	395	394
λ_{PL} (nm)[c)]	444	450	451	454	457	470	470	501	525
ν_a-ν_f (cm^{-1})[d)]	2858	3094	3079	3354	3498	4040	2976	5356	6333

[a)]Polarity factors. [b)]Maximum absorption wavelength. [c)]Maximum emission peak.
[d)]Stokes shift.

Table S2 The PLQYs, lifetimes and radiative transiton rate constants of TPAAnPI.

Solvents	n-hexane	isopropyl ether	diethyl ether	tetrahydrofuran	acetonitrile
Φ(%)[a)]	54.0	53.8	57.7	71.4	58.3
τ(ns)[b)]	1.26	2.16	1.19	2.27	3.76
Kr(s^{-1})[c)]	$4.3*10^8$	$2.5*10^8$	$4.9*10^8$	$3.1*10^8$	$1.5*10^8$

[a)]PLQY. [b)]Lifetime. [c)]Radiative transition rate constant.

Table S3 The energy level and data summary of TPAAnPI from DFT.

	Singlet states			Triplet states	
	Energy level (eV)	Oscillator strength	Dipole moment (Debye)	Energy level (eV)	Dipole moment (Debye)
1	3.4689	0.5449	4.1595	2.1208	4.1285
2	4.0426	0.0002	4.1184	3.1890	2.8141
3	4.0705	0.0013	27.3860	3.5763	6.0637
4	4.1132	0.4936	4.0191	3.6285	4.5457
5	4.3053	0.2878	2.0611	3.6690	4.1495
6	4.4463	0.0198	4.6168	3.7048	4.1333
7	4.4741	0.3820	11.0090	3.7578	4.1159
8	4.4830	0.0622	8.7009	3.8195	6.5104
9	4.5509	0.0033	20.9292	3.8623	4.1148
10	4.5549	0.2590	5.5081	3.9621	4.6466
11	4.7421	0.1143	/	3.9845	/
12	4.8211	0.1745	/	4.0692	/
13	4.9671	0.0221	/	4.2443	/
14	5.0002	0.0810	/	4.2771	/
15	5.0515	0.0402	/	4.3103	/

Table S4. Recent representative non-doped blue OLEDs with $CIE_y \approx 0.2$ based on organic fluorescent small molecules.

Materials	V_{on} [V][a)]	CE_{max} [cd A^{-1}][b)]	EQE_{max} [%][c)]	PE_{max} [lm W^{-1}][d)]	λ_{EL} [nm][e)]	CIE (x, y)	L_{max} [cd m^{-2}][f)]	ref
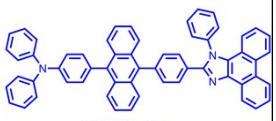 **TPAAnPI**	3.4	18.09	11.47	12.35	470	0.15, 0.22	29900	This work
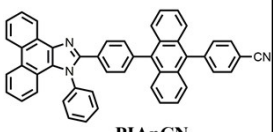 **PIAnCN**	3.0	13.16	9.44	/	470	0.14, 0.19	57787	1
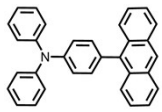 **TPA-AN**	_	5.06	3.0	2.48	460	0.15, 0.23	10079	2
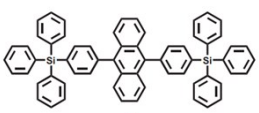 **2**	-	3.26	2.05	2.92	454	0.18, 0.18	1487	3

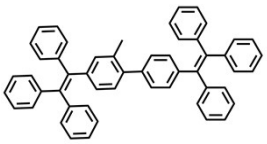 mMethylTPE-pTPE	4.0	8.4	2.60	-	452	0.18, 0.21	11668	4
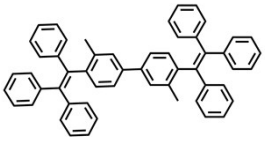 oMethyl-BTPE	4.0	6.7	1.57	-	450	0.18, 0.18	8685	4
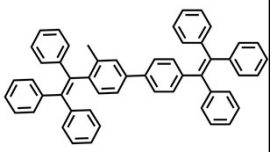 oMethylTPE-pTPE	3.5	9.7	4.06	_	454	0.17, 0.21	14644	4
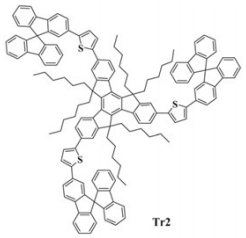 Tr2	4.3	3.88	1.68	1.33	436/464/ 492	0.18, 0.22	11629	5
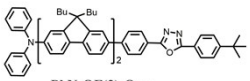 PhN-OF(2)-Oxa	4.0	4.61	3.09	-	460	0.17, 0.19	14747	6
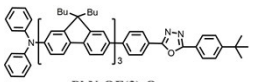 PhN-OF(3)-Oxa	4.0	3.65	2.27	-	470	0.17, 0.23	7707	6
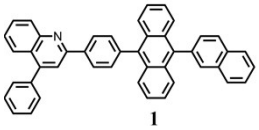 1	-	0.93	-	1.01	460	0.18, 0.23	1525	7
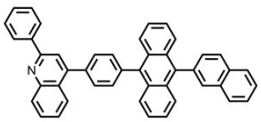 2	-	1.59	-	1.46	451	0.17, 0.21	2011	7
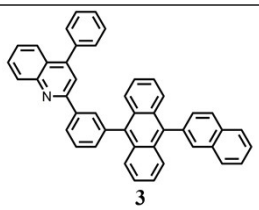 3	-	1.12	-	0.93	445	0.17, 0.19	1303	7
 BDNPA	-	5.21	-	-	-	0.16, 0.19	1300	8

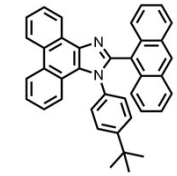 Anthracene-PI	3.2	1.33	0.80	0.97	472	0.16, 0.24	-	9
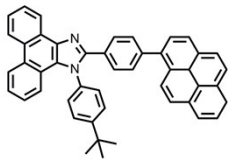 Py-BPI	2.5	3.27	2.07	3.17	468	0.15, 0.18	-	9
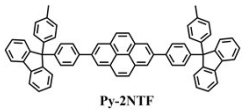 Py-2NTF	3.9	2.50	1.37	1.37	456	0.17, 0.18	6081	10
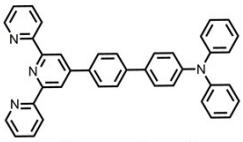 Chromophore I	7.0	0.28	-	-	460	0.19, 0.22	279	11
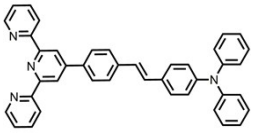 Chromophore II	6.0	-	-	-	466	-	160	11
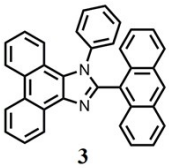 3	3.5	3.43	2.29	-	460	0.16, 0.18	35600	12
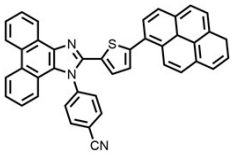 Py-TPICN	3.6	3.00	1.34	2.62	440	0.15, 0.18	14592	13
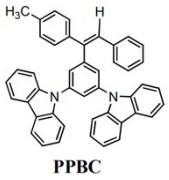 PPBC	-	1.29	-	1.34	441	0.21, 0.22	7500	14
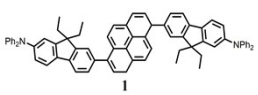 1	-	2.25	1.85	0.92	478	0.17, 0.24	14565	15
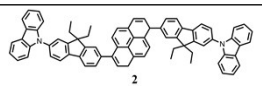 2	-	2.13	1.23	1.03	465	0.16, 0.23	6163	15
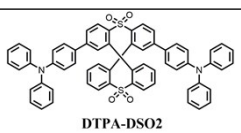 DTPA-DSO2	4.5	9.1	6.3	5.4	-	0.14, 0.22	-	16

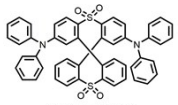 DBPA-DSO2	3.0	6.5	4.7	6.8	-	0.17, 0.22	-	16
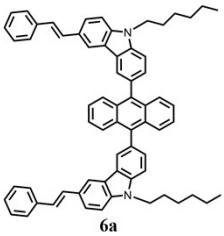 6a	-	4.3	2.8	-	-	0.16, 0.21	-	17
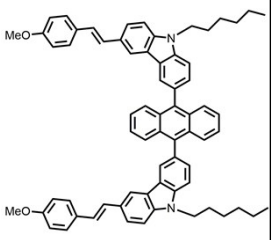 6b	-	4.2	2.6	-	-	0.16, 0.22	-	17
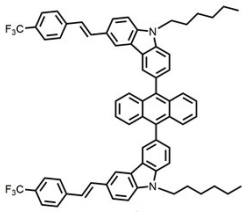 6c	-	1.7	2.4	-	-	0.15, 0.18	-	17
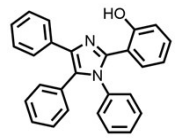 TSPI-1	3.77	-	-	-	457	0.17, 0.18	1.6	18
 BPPI	2.8	6.87	4.0	6.2	468	0.16, 0.21	-	19
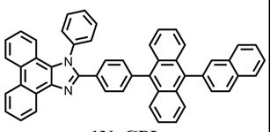 1NaCPI	2.73	4.32	2.82	2.46	-	0.16, 0.20	-	19
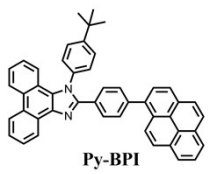 Py-BPI	2.5	3.27	2.07	3.17	-	0.15, 0.18	-	19

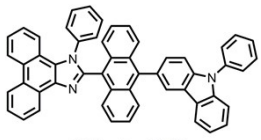 PCz-An-PPI	2.6	6.43	3.99	6.23	-	0.15, 0.23	-	19
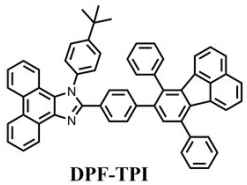 DPF-TPI	2.7	8.41	4.85	7.23	-	0.17, 0.24	-	19
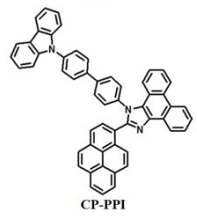 CP-PPI	5.91	3.51	2.39	-	458	0.18, 0.21	-	20

[a)]Turn on voltage at the luminescence of 1 cd m^{-2}. [b)]Maximal current efficiency. [c)]EQE_{max}: Maximal external quantum efficiency. [d)]Maximal power efficiency. [e)]Maximal EL peak value. [f)]Maximum luminescence.

References

1 X. Y. Tang, Q. Bai, T. Shan, J. Y. Li, Y. Gao, F. T. Liu, H. Liu, Q. M. Peng, B. Yang, F. Li and P. Lu, *Adv. Funct. Mater.,* 2018, **28**, 1705813.

2 W. J. Li, Y. Y. Pan, L. Yao, H. C. Liu, S. T. Zhang, C. Wang, F. Z. Shen, P. Lu, B. Yang and Y. G. Ma, *Adv. Opt. Mater.,* 2014, **2**, 892-901.

3 J. Y. Song, S. J. Lee, Y. K. Kim and S. S. Yoon, *Materials Research Bulletin,* 2014, **58**, 145-148.

4 J. Huang, M. Yang, J. Yang, R. L. Tang, S. H. Ye, Q. Q. Li and Z. Li, *Org. Chem. Front.,* 2015, **2**, 1608-1615.

5 C. L. Yao, Y. Yu, X. L. Yang, H. M. Zhang, Z. Huang, X. B. Xu, G. J. Zhou, L. Yue and Z. X. Wu, *J. Mater. Chem. C,* 2015, **3**, 5783-5794.

6 X. J. Feng, J. H. Peng, Z. Xu, R. R. Fang, H. R. Zhang, X. J. Xu, L. D. Li, J. H. Gao and M. S. Wong, *ACS Appl. Mater. Interfaces* **2015**, *7*, 28156.

7 S. N. Park, S. B. Lee, C. Kim, H. W. Lee, Y. K. Kim and S. S. Yoon, *Jpn. J. Appl. Phys.,* 2015, **54**, 06FK06.

8 S. Sohn, M.-J. Kim, S. Jung, T. J. Shin, H.-K. Lee and Y.-H. Kim, *Organic Electronics,* 2015, **24**, 234-240.

9 Y. Zhang, J.-H. Wang, G. Y. Han, F. Lu and Q.-X. Tong, *RSC Adv.,* 2016, **6**, 70800-70809.

10 J. Yang, L. Li, Y. Yu, Z. C. Ren, Q. Peng, S. H. Ye, Q. Q. Li and Z. Li, *Mater. Chem. Front.,* 2017, **1**, 91-99.

11 C. B. Fan, X. M. Wang and J. F. Luo, *Optical Materials,* 2017, **64**, 489-495.

12 T. Shan, Z. Gao, X. Y. Tang, X. He, Y. Gao, J. Y. Li, X. Y. Sun, Y. L. Liu, H. C. Liu, B. Yang, P. Lu and Y. G. Ma, *Dyes and Pigments,* 2017, **142**, 189-197.

13 J. Jayabharathi, P. Jeeva, V. Thanikachalam and S. Panimozhi, *Journal of Photochemistry and Photobiology A: Chemistry,* 2017, **346**, 296-310.

14 H. P. Shi, S. J. Wang, L. Y. Qin, C. Gui, X. L. Zhang, L. Fang, S. M. Chen and B. Z. Tang, *Dyes and Pigments,* 2018, **149**, 323-330.

15 K. Jisu, P. Soyoung, H. Namhee, L. S. Eun,, K. Y. Kwan and Y. S. Soo, *Molecular Crystals and Liquid Crystals,* 2018, **662**, 9-17.

16 D. C. Chen, K. K. Liu, X. L. Li, B. B. Li, M. Liu, X. Y. Cai, Y. G. Ma, Y. Cao and S. J. Su, *J. Mater. Chem. C,* 2017, **5***,* 10991-11000.

17 G. Haykir, M. Aydemir, S.H. Han, S. Gumus, G. Hizal, J.Y. Lee, F. Turksoy, *Organic Electronics* **2018**, *59*, 319.

18 S. L, R. B. Yathirajula, P. Gopikrishna, E. Elaiyappillai, B. A, S. M. S, P. K. Iyer, P. M. Johnson, *Journal of Photochemistry & Photobiology A: Chemistry,* 2018, **365**, 232-237.

19 J. Tagare and S. Vaidyanathan, *J. Mater. Chem. C,* 2018, **6**, 10138-10173.

20 Y. Sim, S. kang, D. Shin, M. Park, K.-Y. Kay and J. Park, *Molecular Crystals and Liquid Crystals,* 2019, **687**, 27-33.